https://doi.org/10.2352/ISSN.2470-1173.2019.9.IMSE-374

Fish-eye Camera Calibration Using Horizontal and Vertical Laser Planes Projected from a Laser Level

Yen-Chou Tai, Yu-Hsiang Chiu, Yi-Yu Hsieh, Yong-Sheng Chen, and Jen-Hui Chuang

Department of Computer Science, National Chiao Tung University, Hsinchu 30010, Taiwan

Abstract

A practical approach to calibrate a fish-eye camera by using horizontal and vertical laser planes projected from a laser level is proposed. The approach does not need to use camera parameters, scene information, and calibration objects in the scene. Instead, only an off-the-shelf laser level is utilized to cast the laser planes toward the scene to generate image features for the calibration based on the principle of projective geometry. With proper alignment of laser level, smooth laser curves can be obtained in the fish-eye image, and the principal center of the camera can be found by intersecting two straight laser lines in the fish-eye image. Other curved laser lines can then be used to measure the calibration data for the correction of radial distortion. Experimental results demonstrate that satisfactory calibration can be achieved by using the proposed method.

1. Introduction

Recently, fish-eye cameras are used in many applications such as vehicle surrounding monitoring, parking assistance system, and indoor security surveillance. Fish-eye cameras are preferable to perspective cameras for large-area monitoring because of their large field of view (FOV), which can be up to 180 degrees or more. Despite the wide FOV, the severe radial distortion of images captured by fish-eye cameras is very difficult for human to perceive. Moreover, for the ever popular multi-view integration, e.g., for car surround view cameras, the above distortions must be corrected beforehand.

Many methods have been proposed to eliminate the radial distortion. The first type of methods utilizes various kinds of calibration apparatuses. Jan and Chang [1] propose to use a calibration object with a concentric and symmetric pattern to determine optical parameters, including the principal point, focal length, and projection function, of fish-eye cameras. Huang et al. [2] provide an image processing apparatus for generating coordination calibration points, which includes a subtraction module, an edge detection module and an intersection point generation module.

The second type of methods is based on a distortion model. In [3], Liu proposes fish-eye image projection-based proportion distortion model. The fish-eye projection principle described in [4] depicts that the distance between a point and the principal center of the image is proportional to the corresponding angle between the incident light and optical axis. This model corresponds to the inverse function of the distortion function and has only two parameters: FOV of the camera and effective maximum radial radius.

Peng [5] proposes a method which does not require any distortion model to calibrate a fish-eye camera, which has a 3-step calibration process: (i) apply ellipse fitting to derive the principal center, (ii) gather calibration data for the radial distortion using a stepping motor, (iii) transform fish-eye image to a perspective one. For (i), details of ellipse fitting can be found in [6] and, similar to several approaches proposed in [7-8], the ellipse center is also identified as the principal center. However, the ellipse center is not the principal center in theory, and location errors will be produced. For (ii), optical axis of the camera is assumed to be perpendicular to the rotation axis of the turntable controlled by the stepping motor. By rotating the turntable with a fixed angle at a time, the calibration data can be obtained by recording consecutive locations of a feature point along radial direction in the image. Although the method presented in [5] is relatively simple, the motor and turntable must be obtained with special orders, while assuring that the above two axes are orthogonal may be an intricate job.

In this paper, we propose to use an off-the-shelf laser level to calibrate a fish-eye camera and acquire necessary data for correcting the radial distortion. The contributions of this paper can be summarized as follows:

(i) While laser level is also used in [9] to find the projection center of a perspective camera, the proposed approach presents an extension for fish-eye camera, and additional calibration for the principal center and the distortion.
(ii) This novel procedure of camera calibration only utilizes an off-the-shelf tool, the laser level, and does not require the deployment of any calibration object in the scene.
(iii) Satisfactory results of calibration can be obtained with the proposed method, as compared with ellipse fitting for the determination of principal center, and compared with OpenCV for the removal of the image distortion.
(iv) With additional off-the-shelf accessory of the laser level, e.g., a computer controllable turntable, adjustment of the rotation angle during the calibration process can be performed automatically.

2. Method for Fish-eye Camera Correction by a Laser Level

2.1. Finding the principal center of a fish-eye camera

In this paper, an off-the-shelf laser level (Ruby-9B4V4H1D), as shown in Fig. 1(a), is employed to calibrate a fish-eye camera. The laser level, as shown in Fig. 1(b), can cast three mutually perpendicular laser planes, with a horizontal one, and can horizontally rotate 360 degrees so as to cast vertical laser planes at different angles. Furthermore, a red point is projected right below the laser level to indicate its ground position.

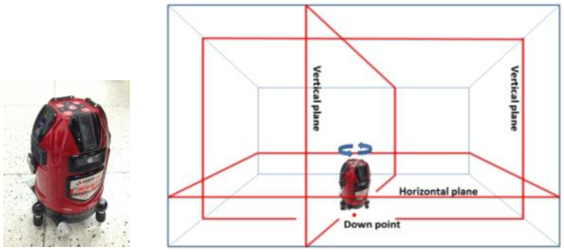

(a) (b)

Figure 1. (a) The laser level (Ruby-9B4V4H1D) used in this paper. (b) Horizontal and vertical laser planes cast by the laser level.

For a laser plane passing through the projection center of the fish-eye camera, the laser line segments in the image will correspond to a smooth curve, which may be segmented due to occlusions. If the laser plane does not pass through the projection center, the laser line segments will neither be connected together nor a smooth curve. Fig. 2 shows images of a vertical laser plane scanning from left to right. In Fig. 2(a) and Fig. 2(c), the laser plane does not pass through the projection center of the camera and the laser line segments in the image do not correspond to a smooth curve. On the other hand, the segments in Fig. 2(b) result in a smooth curve for the laser plane is passing through the projection center. Besides, three laser planes in Fig. 3 also scan from left to right and all of them pass through the projection center because of smooth curves in the image, but only Fig. 3(b) passes through the principal center of the fish-eye camera for the laser line segments correspond to a straight line. In other words, smooth laser curves in fish-eye image indicate that the curves pass the projection center, and only straight laser line passes the principal center. In this article, we use straight laser lines to find the principal center and smooth laser curves to obtain correction data of a fish-eye camera.

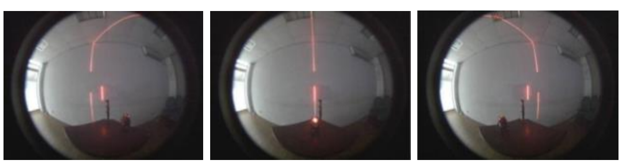

(a) (b) (c)

Figure 2. A laser plane passing through the projection center of a fish-eye camera corresponds to a smooth curve in the image.

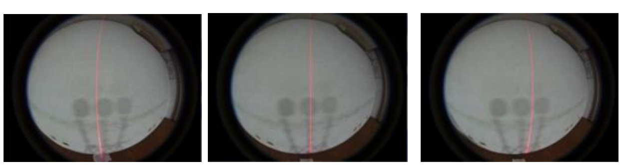

(a) (b) (c)

Figure 3. A laser plane passing through the principal center of fish-eye camera gives a straight line in the fish-eye image.

In the proposed approach, two straight laser lines will be utilized to find the principal center of a fish-eye camera, with one of them corresponding a vertical laser plane, as shown in Fig. 3(b). For the other laser line, the procedure discussed in the following will identify the horizontal laser plane which is passing through the projection center as well as the principal center of the camera. One way of finding such a laser line is to keep the laser level fixed in location and alternately adjusting the height and pitch of the fish-eye camera. For example, if the laser line in the image does not correspond to a smooth curve, as shown in Fig. 4(a), the camera height will be adjusted manually for a smooth one as shown Fig. 4(b). Subsequently, the pitch of the camera will be adjusted according to the monotonically varied convexity of the curve, and followed by iterations of height adjustment until a straight laser line is obtained in the image as shown in Fig. 4(c). Finally, we place the laser level outside the FOV of the fish-eye camera and then use the above processes, the horizontal laser plane is found as shown in Fig. 4(d). Furthermore, all calibration processes can be performed automatically by a computer controllable turntable.

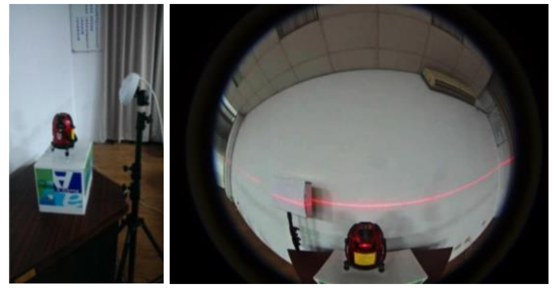

(a) A laser line without smoothness in the fish-eye image.

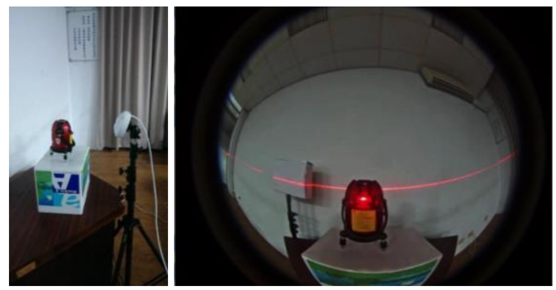

(b) A laser line corresponds to a smooth curve in the image.

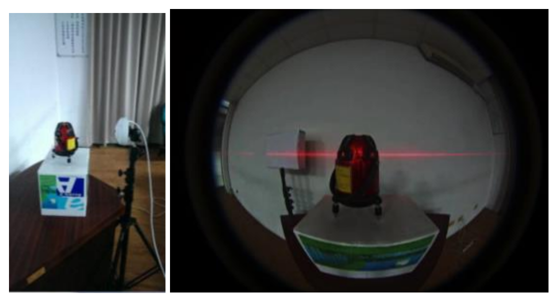

(c) A straight laser line in the image implies the laser plane passing through the principal center of the camera.

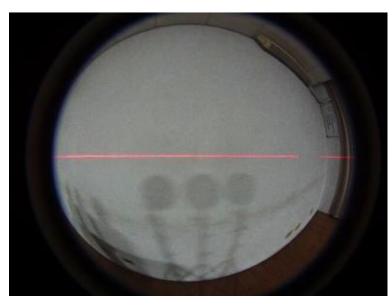

(d)

Figure 4. Adjusting the fish-eye camera to obtain a straight laser line in the fisheye image.

After vertical and horizontal laser lines are obtained by proposed method as shown in Figs. 5(a) and (d), the principal point can be estimated. Because the laser planes could be dark when the scene is in the adequate light, we solve this problem by using HSV color model and adjusting the values of Hue, Saturation, and Value to reveal laser lines [9]. As the laser line is extracted with image pixels and may be fractured (Figs. 5(b) and (e)), equations of both vertical and horizontal laser lines are first estimated using the least squares method as shown in Figs. 5(c) and (f). The intersection of the two lines is then identified as the principal point of the fish-eye image.

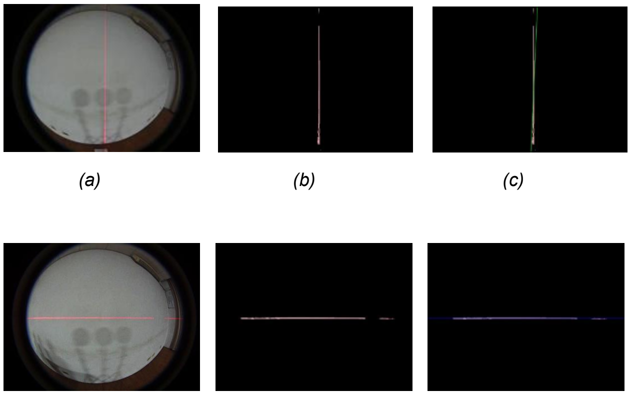

(a) (b) (c)

(d) (e) (f)

Figure 5. The processes of finding vertical and horizontal laser lines for the computation of the principal point of the fish-eye image. (a) and (d): The vertical and horizontal laser lines obtained by proposed method. (b) and (e): the laser line extracted from image pixels (a) and (d), but fractured. (c) and (f): The vertical and horizontal laser line found and depicted in green line and blue line, respectively.

2.2. Measuring calibration data of a fish-eye camera

In this section, a laser level is used to assist the acquisition of the calibration data. The goal is to record from the fish-eye image the (radial) displacement of intersections of (i) vertical laser planes (laser curves) and (ii) the horizontal plane (line) derived above, for selected angular positions of (i) with respect to the projection center. For the special case shown in Fig. 5(a), which corresponds to an angle of zero degree, the curve in (i) becomes a straight line. To correct the radial distortion, e.g., for an ordinary perspective projection, the above displacement will then be adjusted accordingly.

With the camera projection center estimated with the procedure developed in the previous subsection, vertical laser planes in (i) can be obtained by first placing the laser level, e.g., on the ground plane, so that the down point coincides the ground projection of the camera projection center. Next, the laser curves can be extracted in the fish-eye image by rotating the laser level for say 10, 20, 30, 40, 50, 60, 70, and 80 degrees, with the line shown in Fig. 5(a) corresponding to an angular position of zero degree. Thus, a total of nine intersections can be obtained for (i) and (ii) mentioned above. Finally, the calibration data can be obtained by calculating the displacement of these intersections from the principal center in the radially distorted image as

$$D(x, y) = \sqrt{(x - u_0)^2 + (y - v_0)^2} \quad (1)$$

where (x, y) is the coordinate of an intersection point, (u_0, v_0) is the coordinate of the principal center, and D is the radial displacement of the intersection point for the angular position of a particular vertical laser plane in (i). Thus, Peng's method [5] can be applied to de-warp the fish-eye image by adjusting image content along radial directions using these calibration data (radial displacements).

3. Experimental Results

We first apply the proposed method to estimate the principal center of fish-eye camera of model AXIS M3007-P. Since the laser has red color, image pixels with Hue between 0 and 20 degrees or 340 and 360 degrees, Saturation between 0.2 and 1.0, and Value between 0.6 and 1.0, are extracted from Figs. 6(a) and (b) for the estimation of horizontal and vertical laser lines, respectively. Then, equations of the two lines are found by the least squares method, as shown in Fig. 6(a), with the principal center being their intersection. Such a calibration result can be compared with that obtained via ellipse fitting, as shown in Fig. 6(b), whereas center of the ellipse is identified as the principal center. Although Table 1 indicates a near 4-pixel difference between the two centers, our approach is based on the principle of projective geometry and will always generate consistent calibration results, while variations in housing assembly of the camera may degrade the quality of the calibration based on ellipse fitting.

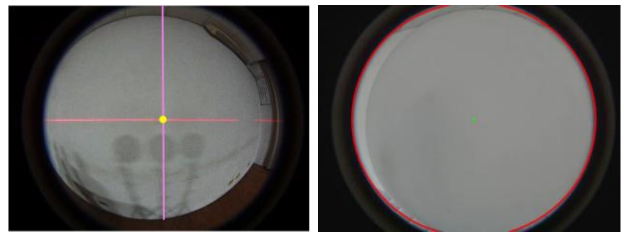

(a) (b)

Figure 6. Estimations of the principal center by using (a) a laser level (yellow point) and (b) the ellipse fitting method (green point).

Table 1. Comparison of the principal centers.

Method	Coordinate of principal center	Difference (pixel)
Laser level	(332.37, 243.01)	(3.62, 0.60)
Ellipse fitting	(328.75, 242.41)	

Next, images of vertical laser planes in different directions, with 10 degrees apart starting from zero degree, are identified in the fish-eye image as smooth laser curves, as shown in Figs. 8(a) to (f). Intersections of these curves and the horizontal line shown in Fig. 5(b) will then be identified as the calibration data mentioned in the previous section.

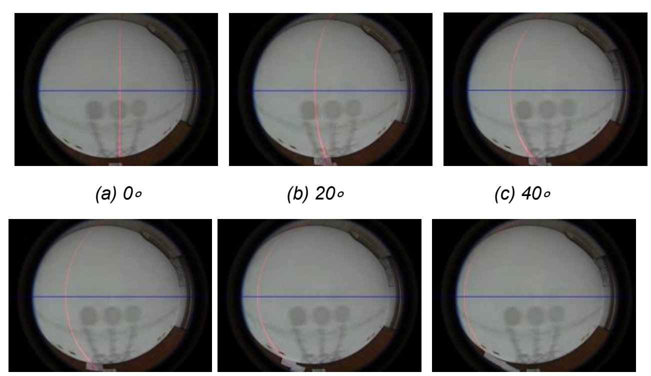

(a) 0∘ (b) 20∘ (c) 40∘

(d) 50∘ (e) 70∘ (f) 80∘

Figure 7. Images of vertical laser planes (red curves) with 0 to 80 degrees in angular position with respect to camera projection center. For brevity, the curves are only depicted for six of the nine equally spaced (in angle) vertical laser planes generated by a laser level.

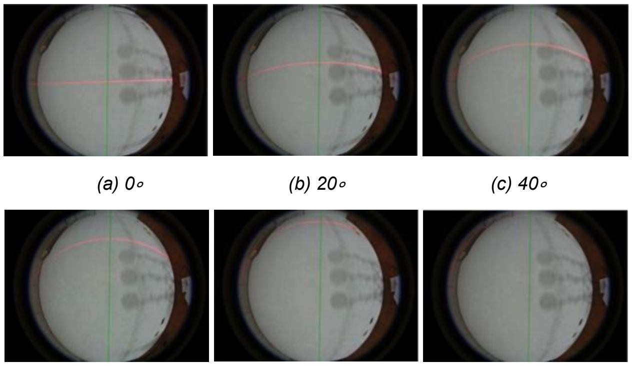

(a) 0° (b) 20° (c) 40°

(d) 50° (e) 70° (f) 80°

Figure 8. Image features similar to those shown in Fig. 7. The calibration is performed for the fish-eye camera rotated (panned) by 90 degrees.

To demonstrate that the proposed calibration can be performed for different camera orientations, and for different radial directions, we rotate (pan) the fish-eye camera by 90 degrees and repeat above procedure, and Fig. 8 shows image features, similar to those shown in Fig. 7, thus obtained. Fig. 9 depicts the horizontal and vertical displacements in the fish-eye image obtained from Figs. 8 and 9, respectively, for different angles of laser plane. Note that differences between the two set of displacement data are less than 3.46 pixels, indicating that the proposed calibration has consistent performance[1].

Eventually, the undistorted image for the fish-eye camera can be obtained using the corresponding calibration data. Figs. 10(a), (b), and (c) show a fish-eye image, its de-warped version obtained with the proposed method, and that from an OpenCV implementation [10], respectively. (The OpenCV approach first utilizes Harris corner detector to extract point features from images of a calibration object (chessboard). Then, intrinsic and extrinsic camera parameters are obtained with algorithms presented in [11] and [12]. Finally, these parameters are used to rectify the image.) Figs. 11, 12, and 13 show similar results but for a different scene. It is readily observable that line features in the scenes are all straightened but with the proposed approach getting slightly better results that those obtained by OpenCV.

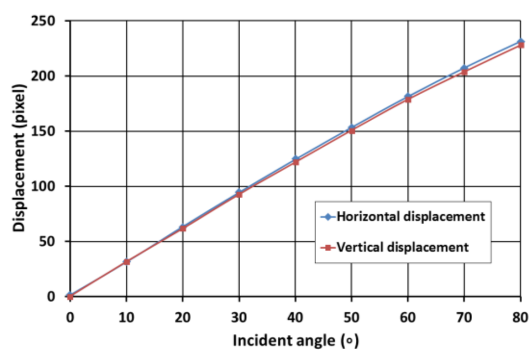

Figure 9. Displacements, from the principal center of a fish-eye image, along two radial directions for different angles of laser planes.

4. Conclusion

In this paper, an off-the-shelf laser level is employed in the development of a calibration procedure for fish-eye cameras. The principal center of the fish-eye image can be identified using the line/curve features obtained by the laser level casting vertical and horizontal planes. The calibration data can be obtained from the intersection of these features, and such data will give displacements of feature points along the radial direction. Since the proposed procedures need neither camera parameters nor scene information, our approach will work for all fish-eye cameras in general. Finally, experimental results depict that the differences in location between the principal center found by the proposed method and that by ellipse fitting are equal to 3.62 pixels. Furthermore, several examples of fisheye images are undistorted via the proposed method and an OpenCV implementation, and the results demonstrate that a fish-eye image camera can be transformed satisfactorily to a perspective one with the proposed calibration procedure.

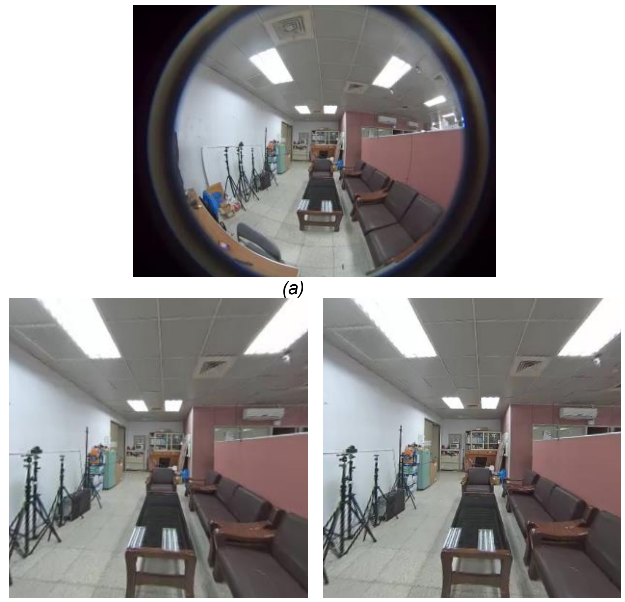

(a)

(b) (c)

Figure 10. Results of de-warping. (a) a 512×512 fish-eye image, (b) image de-warped with the proposed approach, (c) image de-warped with OpenCV.

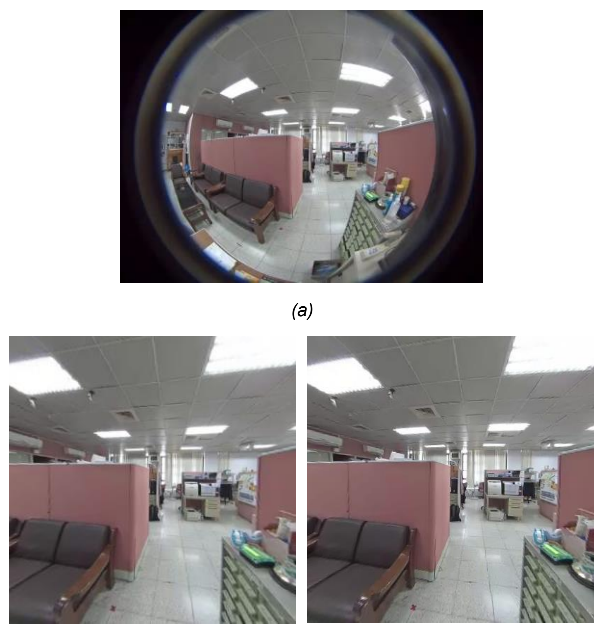

(a)

(b) (c)

Figure 11. Another example of de-warping. (a) a 512×512 fish-eye image, (b) image de-warped with the proposed approach, (c) image de-warped with OpenCV.

[1] Nonetheless, such an observation also depends on whether the image has perfect circular symmetry.

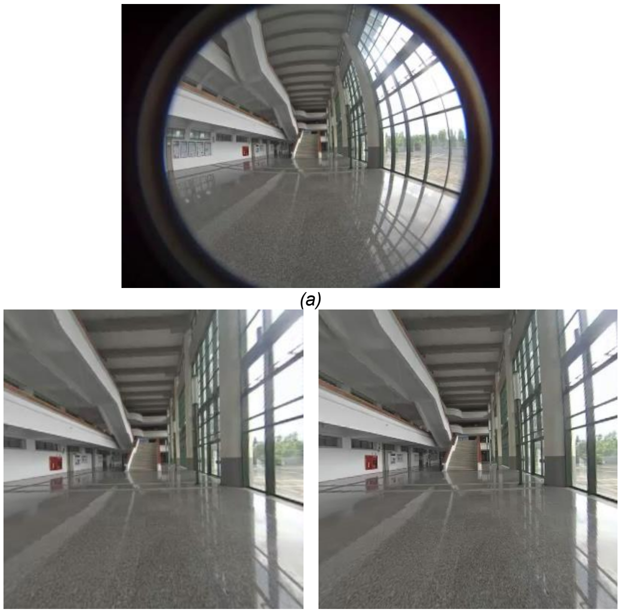
(a) (b) (c)

Figure 12. Another scene of de-warping. (a) a 512×512 fish-eye image, (b) image de-warped with the proposed approach, (c) image de-warped with OpenCV.

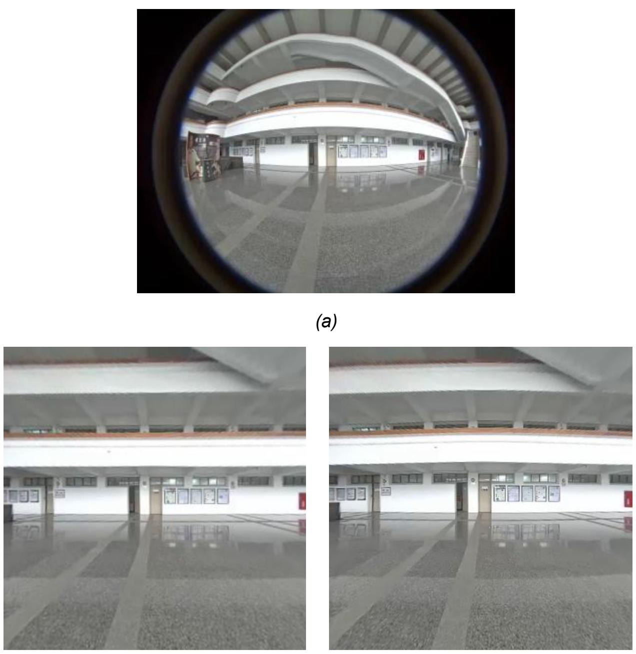
(a) (b) (c)

Figure 13. Another example of de-warping. (a) a 512×512 fish-eye image, (b) image de-warped with the proposed approach, (c) image de-warped with OpenCV.

References

[1] G.-J. Jan and C.-J. Chang, "Method for presenting fisheye camera images", U.S. Patent 7 042 508, May, 9, 2006.

[2] Y.-M Huang, C.-C. Chiang, and Y.-C. Liu, "Image processing apparatus and method for generating coordination calibration points", U.S. Patent 8 275 191, September, 25, 2012.

[3] Y.-C. Liu, "Fisheye camera calibration and multiple-viewpoint image stitching," M.S.Thesis, National Chiao Tung University, Hsinchu, Taiwan, 2007.

[4] F. Devernay and O. Faugeras, "Straight lines have to be straight: Automatic calibration and removal of distortion from scenes of structured environments," *Machine Vision and Applications*, vol. 13, pp.14–24, 2001.

[5] C.-K. Peng, "Camera calibration and image stitching of vehicle surrounding monitoring system," M.S.Thesis, National Chiao Tung University, Hsinchu, Taiwan, 2014.

[6] A. Fitzgibbon, M. Pilu, and R. B. Fisher, "Direct least square fitting of ellipses," *IEEE Transactions on Pattern Analysis and Machine Intelligence*, vol. 21, no.5, pp.476-480, 1999.

[7] Branislav Micusik and Tomas Pajdla, "Estimation of omnidirectional camera model from epipolar geometry," *IEEE Conference on Computer Vision and Pattern Recognition*, vol. 1, pp. 485-490, 2003.

[8] J. Kannala and S. Brandt, "A generic camera calibration method for fish-eye lenses," *IEEE Conference on Pattern Recognition*, vol. 1, pp. 10-13, 2004.

[9] Y.-C. Tai, C.-W. Liu, Y.-S. Chen, and J.-H. Chuang, "Efficient calibration for multi-plane homography using a laser level," *IEEE Conference on Image Processing,* pp. 2010-2014, 2015.

[10] OpenCV documentation (Sep 11, 2016). *Camera Calibration and 3D Reconstruction* [Online]. Available:http://docs.opencv.org/2.4/modules/calib3d/doc/camera_calibration_and_3d_reconstruction.html

[11] Z. Zhang, "A flexible new technique for camera calibration," *IEEE Transactions on Pattern Analysis and Machine Intelligence,* 22(11):1330-1334, 2000.

[12] J.-Y. Bouguet, *MATLAB calibration tool* [Online]. Available: http://www.vision.caltech.edu/bouguetj/calib_doc/